Progress in Physics of Applied Materials 2 (2022) 165–173

Semnan University

Progress in Physics of Applied Materials

journal homepage: https://ppam.semnan.ac.ir/

$CoFe_2O_4$ bulk, nanoparticles and layer: A comparison of structural, magnetic, and optical properties

S. Sayyar, B. Aslibeiki*, A. Asgari

Faculty of Physics, University of Tabriz, Tabriz, Iran

ARTICLE INFO

Article history:
Received: 27 November 2022
Revised: 18 December 2022
Accepted: 24 December 2022

Keywords:
Cobalt ferrite
X-ray diffraction
Magnetization
Coercivity
Band gap

ABSTRACT

The structural characteristics of materials change with the reduction of dimensions, and they show different behaviors compared to the corresponding bulk sample. To study these changes, in this research, we investigated the effect of size and preparation method on properties of cobalt ferrite ($CoFe_2O_4$). After synthesis of a bulk sample by solid-state reaction method, $CoFe_2O_4$ nanoparticles were prepared by two different methods of co-precipitation and thermal decomposition. Then, a layer of $CoFe_2O_4$ was prepared by a spin coating method, using a silicon substrate. In the following, the structural, magnetic, and optical properties of samples were studied, and compared. The results confirmed the size and synthesis method dependence behavior of properties of the prepared samples. The nanoparticles synthesized by thermal decomposition method show much higher coercivity compared to those prepared by co-precipitation, while both consist of almost same size distribution. The bulk sample shows the lowest coercivity, but highest saturation magnetization among the samples. On the other hand, the bulk sample has smaller band gap compared to the nanoparticles.

1. Introduction

Spinel ferrites are a group of magnetic materials with the chemical formula of MFe_2O_4, whose main part of the structure is iron (III) oxide. Cobalt ferrite ($CoFe_2O_4$) is a hard ferrite with an inverse cubic spinel structure. The $CoFe_2O_4$ has characteristics such as high anisotropy and coercivity, moderate saturation magnetization, and chemical and physical stability [1-3]. Some of the applications of $CoFe_2O_4$ include recording media, data storage, sensors, the automotive industry, and microwave devices [4-7]. The magnetic properties of this material are highly size and morphology dependent [8-10]. By changing these quantities, the properties can be controlled to achieve a desired application. Studies show that the saturation magnetization reduces by decreasing the size of particles. This reduction is mainly due to the surface spin canting and formation of a paramagnetic shell called dead layer [11]. Different attempts have been reported to reduce the negative effect of dead layer on magnetization of ferrite nanoparticles. As an example, coating the particles with some polymers can reduce the paramagnetic disorder and improve the magnetization [12-14]. In addition to the magnetization, the coercivity is one of the most important futures of the $CoFe_2O_4$. This parameter depends on the size, morphology, and synthesis method. Controlling the coercivity by doping of Fe and Mn in $CoFe_2O_4$ structure was reported in literature [15, 16]. Beside the nanoparticles, the $CoFe_2O_4$ layer can be prepared by different coating methods. One of simple methods is spin-coating using solution containing ferrite nanoparticles [17]. The bulk sample shows different properties compared to layer and nanoparticles. One of the properties that strongly depends on the size and morphology is the optical properties. The band gap is a size dependent parameter and by reducing the dimension and size, an increase in band gap of the material is expected. As the best of our knowledge, there are no reports in literatures on the study and comparing the physical properties of $CoFe_2O_4$ bulk sample with its other morphologies (nanoparticles, layer, etc.). Since the application of a material strongly depends on its properties, and the characteristic of a sample is size and morphology dependent parameter, therefore, in this research study, $CoFe_2O_4$ was prepared in three forms of nanoparticles; layer

* Corresponding author
E-mail address: b.aslibeiki@tabrizu.ac.ir

DOI: 10.22075/ppam.2022.29079.1047

and bulk sample, and structural, magnetic, and optical properties of samples were compared.

2. Materials and Experimental

2.1. Materials

Raw materials including $FeCl_3.6H_2O$, $CoCl_2.4H_2O$, NaOH. $CoN_2O_6.6H_2O$, $FeN_3O_9.9H_2O$ and $C_6H_8O_7$, Polyvinylpyrrolidone, Co_3O_4 and Fe_3O_4 powders where purchased from Merck Co.

2.2 Preparing the $CoFe_2O_4$ nanoparticles by co-precipitation method

In this method, $FeCl_3.6H_2O$, $CoCl_2.4H_2O$ as metal salts, and NaOH as precipitation agent were used. After obtaining the stoichiometric values, the mixture of metal salts and sodium hydroxide were dissolved separately in deionized water. Then, the temperature of the metal salts solution was raised to 80 °C, and sodium hydroxide solution was added to it. The stirring continued for 30 minutes at a constant temperature of 80 °C. Then, using a strong magnet, we washed the sediments with deionized water and the obtained nanoparticles were dried at room temperature.

2.3. Preparing the $CoFe_2O_4$ nanoparticles by thermal-decomposition method

To prepare nanoparticles by thermal decomposition method, $CoN_2O_6.6H_2O$, $FeN_3O_9.9H_2O$, and $C_6H_8O_7$ were used. After determining specific amounts, cobalt nitrate, iron nitrate, and citric acid were mixed uniformly. Then the mixture was placed in the oven at 500 °C for one hour.

2.4. Preparing the $CoFe_2O_4$ layer on Si substrate

Cobalt ferrite nanoparticles were used to synthesize the cobalt ferrite layer on a silicon substrate. All the preparation steps of nanoparticles were done according to co-precipitation method. At the end of synthesis, instead of drying, nanoparticles were dissolved in Polyvinylpyrrolidone (PVP) solution in ethanol with a concentration of 10 mg/ml. In the end, a spin coating machine was used at a speed of 1000 rpm and for 20 seconds, and a layer was prepared.

2.5. Preparing the bulk $CoFe_2O_4$ sample

To prepare a bulk sample of cobalt ferrite, high-purity commercial Co_3O_4 and Fe_3O_4 powders have been used. After specifying the stoichiometric values, the above chemicals were mixed and then the resulting mixture was made into tablets and annealed at 1350 °C for 24 hours.

2.6. Instruments

In the first part, the structural properties are studied using instruments such as X-ray diffractometer (XRD model Tongda TD-3700), field emission scanning electron microscope (FE-SEM model TESCAN MIRA3), and Fourier transform infrared spectrometer (FTIR model TENSOR 27). In the second part, a vibrating sample magnetometer (VSM with H_{max}=±15 kOe, model Meghnatis Daghigh Kavir Co., Iran) was used to study the magnetic properties of the samples. In the third part, UV-Vis (UV-Vis model Shimadzu UV-2450) spectrometer was used to study the optical properties.

3. Results and discussion

3.1. Structural properties

Fig. 1(a) shows the X-ray diffraction pattern of nanoparticles in the range of 2θ: 10-100°. This pattern confirms that the cobalt ferrite nanoparticles have been synthesized by thermal decomposition (T) and co-precipitation (C) methods, and the resulting patterns indicate the formation of Fd-3m cubic spinel structure (card No. 022-1086). The XRD pattern of the bulk sample is shown in Figure 1(b) that corresponds to standard ICDD card number of 1086-022. By comparing the XRD patterns in Figures 1(a), and 1(b), it can be seen that the peaks in the bulk sample are sharper with higher intensity. This means that the degree of crystallinity is higher in the bulk sample. The XRD pattern obtained from the layer of cobalt ferrite is drawn in the range of 20-80°, and can be seen in Figure 1(c). This pattern is consistent with the powder diffraction data of the standard card number of 003-0864. The two additional sharp peaks at the angle of 68.62° and one peak with low intensity at the angle of 33.49° are observed, which are due to the crystalline structure of the silicon wafer substrate. To calculate lattice constant (a), and unit cell volume ($V_{u.c}$), following equations were used [18]:

$$a = d\sqrt{h^2 + k^2 + l^2} \quad (1)$$

where, d is the distance between Bragg planes, and h, k, and l are Miller indices. Also, the crystallite size is calculated from the Scherrer equation [19]:

$$D = \frac{k\lambda}{\beta \cos\theta} \quad (2)$$

where, D is the size of crystallites, k is Scherer's constant (which is related to the shape of nanoparticles and is equal to 0.9), λ is the wavelength of X-ray (0.15406 nm), β is the peak width at half maximum intensity (FWHM), and θ is the Bragg angle. Considering that there are eight chemical formula units in each unit cell, the density of prepared nanoparticles can also be calculated. In this regard, M is the molecular mass of $CoFe_2O_4$ and N_A is Avogadro's number [18]:

$$\rho = \frac{8M}{N_A V} \quad (3)$$

The results obtained from applying equations 1, 2, and 3 are collected in Table 1 The crystallite size, and the values of the lattice constant, unit cell volume, and density for nanoparticles and Bulk samples are in good agreement

with each other and literatures [20-22]. The lattice constant of the layer is slightly higher than that of the Bulk standard sample (8.39 Å). This result indicates a tensile strain in the lattice concerning the silicon wafer substrate [23].

To study the morphology and nanoparticles size, FE-SEM image was also prepared from the samples. Figure 2 (a,d) shows the images obtained from FE-SEM of samples with the corresponding particle size distribution fitted with normal logarithmic function [24]:

$$f(D) = \frac{1}{\sqrt{2\pi}\sigma D} \exp\left[-\frac{ln^2\left(\frac{D}{D_0}\right)}{2\sigma^2}\right], \quad (4)$$

where D_0 is the median diameter and σ is the dispersion. The mean diameter $\langle D \rangle = D_0 \cdot \exp(\sigma^2/2)$ and standard deviation $\sigma_D = \langle D \rangle \cdot [\exp(\sigma^2) - 1]^{1/2}$ were determined using the fit parameters D_0 and σ. According to the images, the synthesized nanoparticles are almost spherical and are found in aggregation in some parts. The average particle size is given in Table 1. By comparing the values in Table 1, we find that the size obtained from the images is larger than that obtained from the Scherrer formula. The nanoparticles may be composed of several crystallites, and therefore the size of the particles will be larger than the size of the crystallites obtained by Scherrer equation [25]. According to Figure 2 (a,b), the aggregation of nanoparticles in the sample synthesized by the thermal decomposition method is higher than that in the sample synthesized by the co-precipitation method. This can be due to the high annealing temperature in the thermal decomposition method, which leads to the formation of bonds in the interfacial regions of the particles. Although there is a tendency for aggregation in all magnetic nanoparticles, it seems that the amount of aggregation is higher in the samples synthesized by annealing in the oven than in the samples synthesized in a liquid phase.

Infrared Fourier transform (FT-IR) analysis was done for the nanoparticles and Bulk sample in the wavelength range of 400-4000 cm^{-1}. The spectrum was performed to ensure the purity of the synthesized samples and the formation of the crystalline phase. The results are shown in Figure 3 By examining the FT-IR spectrum of spinel ferrites, it can be seen that there are two peaks at wavelengths below 600 cm^{-1}, which are related to the spinel structure of cobalt ferrite [26, 27]. The first peak in the range of 425-435 cm^{-1} is related to the bond of oxygen-metal Fe^{3+} and (Co^{2+}) in the octahedral position, and the second peak in the range of 579-585 cm^{-1} is related to the bond of oxygen-metal (Fe^{3+}) in the tetrahedral position [28]. In thermally decomposed nanoparticles, we see the peak at 1326 cm^{-1}, which is related to the stretching vibration of C=O. Also, the peak at 1510 cm^{-1} is related to the N-H bond. These two peaks can be related to impurities of the used KBr. The absorptions related to the vibrations of the H-O-H water bonds occurred at the wavelength of 1618 cm^{-1}. The broad peak located at 3394-3394 cm^{-1} is related to the bonds of O-H water molecules [29, 30].

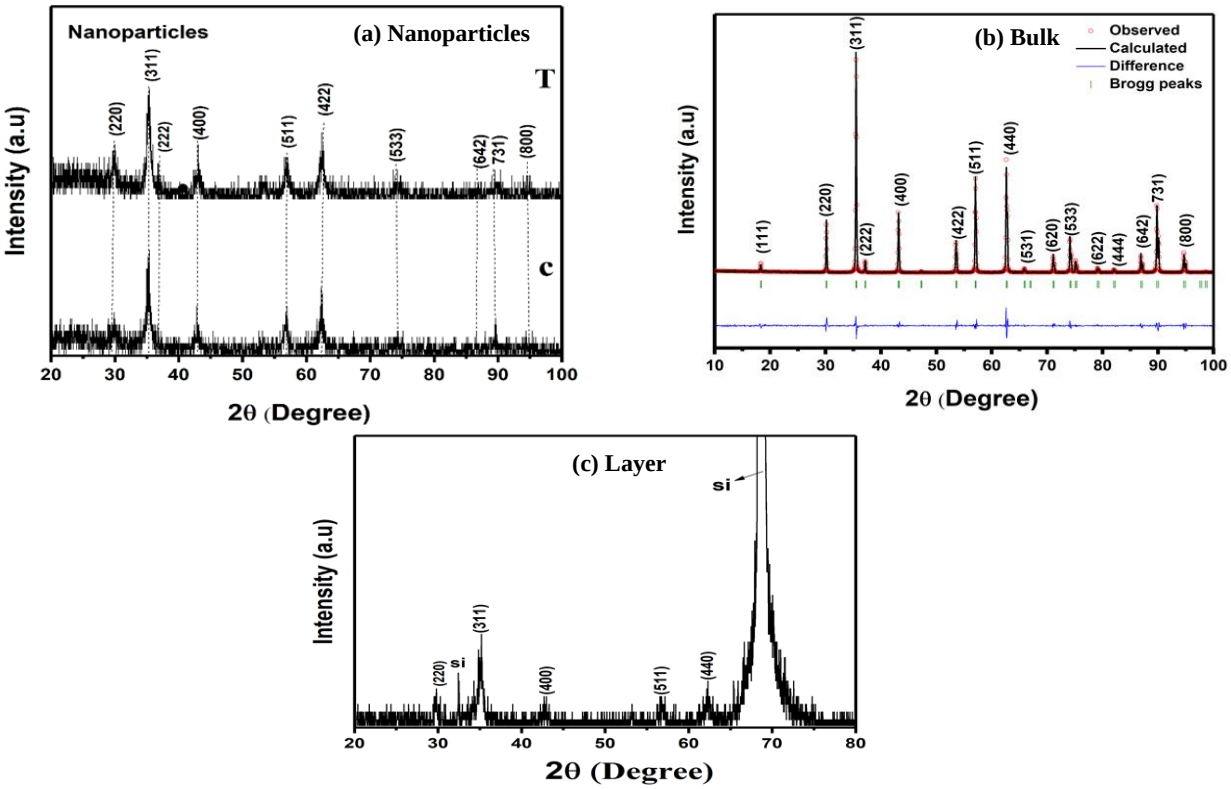

Fig. 1. XRD patterns of the samples.

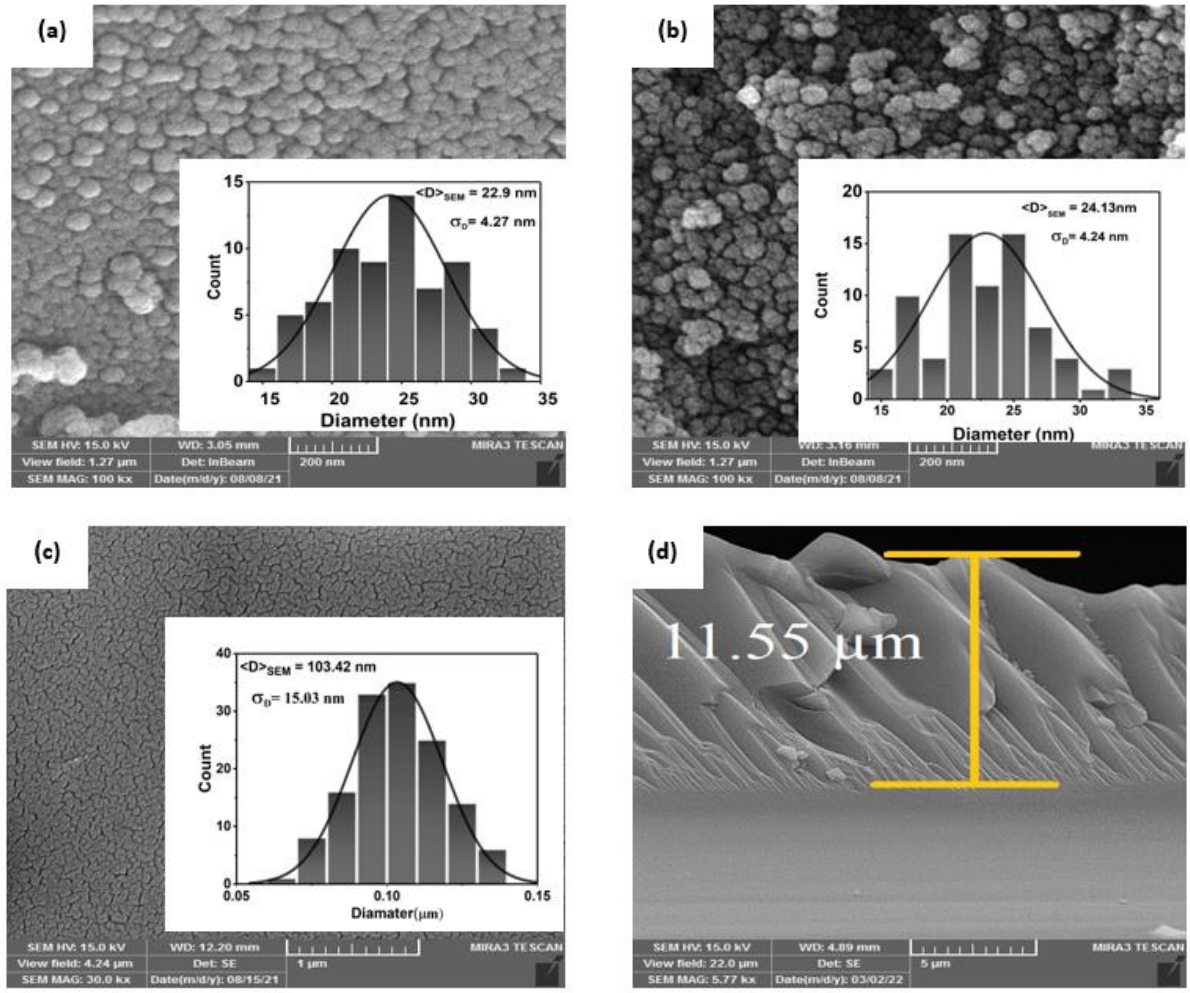

Fig. 2. FE-SEM micrographs of (a) Thermal decomposition nanoparticles, (b) Co-precipitation nanoparticles, (c) bulk sample with corresponding particle size histogram fitted with a log-normal function, and (d) layer of $CoFe_2O_4$.

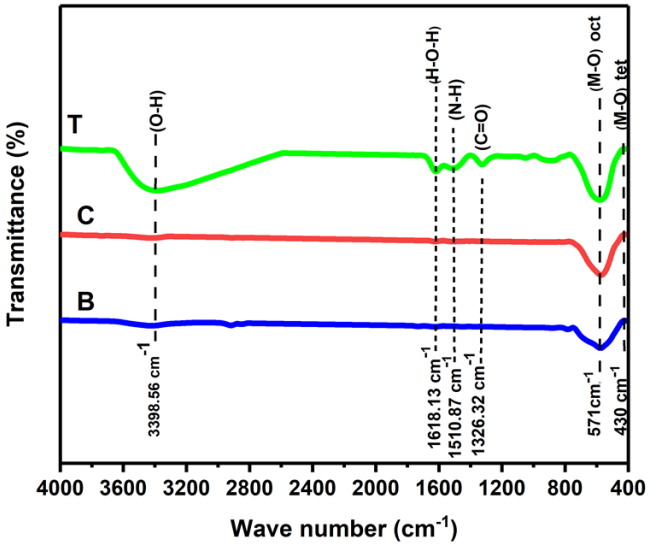

Fig. 3. FTIR spectra of the samples.

Table 1. Lattice constant (a), the volume of unit cell ($V_{u.c}$) of nanoparticles and bulk $CoFe_2O_4$, density (ρ), average crystallites size $\langle D\rangle_{XRD}$, and mean particles size obtained by FE-SEM $\langle D\rangle_{SEM}$.

Parameter	C	T	L	B
a (Å)	8.40±0.03	8.38±0.05	8.44±0.02	8.38
$V_{u.c}$ (Å^3)	594.08± 8.28	589.87±11.98	601.84±4.45	588.51
ρ (g/cm^3)	5.24	5.28	5.17	5.29
$<D>_{XRD\text{ - }Scherrer}$ (nm)	17.72±6.08	13.08±3.39	16.95±7.49	-
$<D>_{SEM}$ (nm) + σ_D (nm)	22.9±4.24	24.13±4.27	34.03±7.18	103.42±15.04

3.2. Magnetic properties

A vibrating sample magnetometer (VSM) was used to study the magnetic properties. The magnetization of the samples was measured in terms of the applied field at room temperature, and the magnetic hysteresis curve was drawn in Figure 4 By studying the hysteresis loops, it is possible to measure various magnetic parameters, which are listed in Table 2. According to Figure 4, the hysteresis loop of all samples shows that cobalt ferrite is a hard ferrite. At first, the saturation magnetization (M_s) of the samples is compared with each other and other references. Among the main factors that change the saturation magnetization in the spinel ferrite, we can mention the distribution of cations in A and B positions of spinel structure, the size of nanoparticles, and the spin irregularities of the shell in small dimensions (nanoparticles) [31, 32]. According to Table 2, the saturation magnetization in the bulk sample is 88.77 (emu/g), which is consistent with literature [6, 33]. The saturation magnetization of nanoparticles is almost same, and similar with literature [12, 16, 34], and the saturation magnetization for the layer equals 122.70 emu/cm^3. This value can convert to emu/g using the layer density or mass. Or for comparison, one can convert the emu/g unit to emu/cm^3 using mass density. If the saturation of the bulk sample is compared with nanoparticles and layer, it can be seen that there is a big difference between them. The reason for the higher saturation magnetization in the bulk sample can be explained by reducing the size of the particles (down to the nanoscale). The more the surface, the properties of nanoparticles change, especially the magnetic properties. As the particle size decreases, the contribution of the surface paramagnetic dead layer in the total magnetization increases and thus causes a decrease in M_s value compared to the bulk sample. The dead layer thickness is obtained from the following equation [35]:

$$M_s = M_s(b)\left[1 - \frac{6t}{d}\right] \quad (5)$$

where, M_S (b) is the saturation magnetization in bulk sample, d is the particle diameter, and t is the thickness of the dead layer. According to Table 3, the thickness of the dead layer for co- precipitation and thermal decomposition nanoparticles are almost close to each other and therefore have the same saturation magnetization. In general, as the size of the particles increases and we get closer to the bulk state, the importance of the effect of the size of the particles and the dead layer decreases, and the change in the distribution of metal cations in the positions of the spinel structure has a greater effect on the saturation magnetization. Among other factors affecting the saturation magnetization of nanoparticles and cobalt ferrite layer, it can be mentioned that, due to the small dimensions (nanoscale), the irregularity of surface spins (caused by oxygen vacancies and broken iron-oxygen or cobalt-oxygen bonds on the surface), and the surface anisotropy has caused their magnetization to be smaller [7]. In addition, by comparing the coercivity (H_c) values (see Fig. 4(a)), it can be seen that for nanoparticles prepared by thermal decomposition method, the H_c is much higher than those prepared by co-precipitation. The first reason is due to the annealing of T sample at 500 °C. That is, by annealing at higher temperatures (up to about 700 °C), a higher coercivity value can be achieved, which is consistent with the literatures [25]. The second reason is the increase of the effective anisotropy constant, which can increase the coercivity value. Effective anisotropy consists of two parts, volume anisotropy and surface anisotropy, which is much more effective in nanoparticles. It is essential to mention that the effect of particle size on the H_c is such that, it increases with the increase of particle diameter and then decreases after reaching a certain value. Therefore, the bulk sample prepared at high temperature has a lower H_c value [36]. Figure 4(b) shows hysteresis loops in two modes of in plane and out of plane. The curves show almost same trend. Since the layer was prepared using nanoparticles solution, therefore, the orientation of easy axis is similar to nanoparticles sample and there is no preferred direction of easy (hard) axis. Then changing the direction of applied field has not noticeable effect on hysteresis loop.

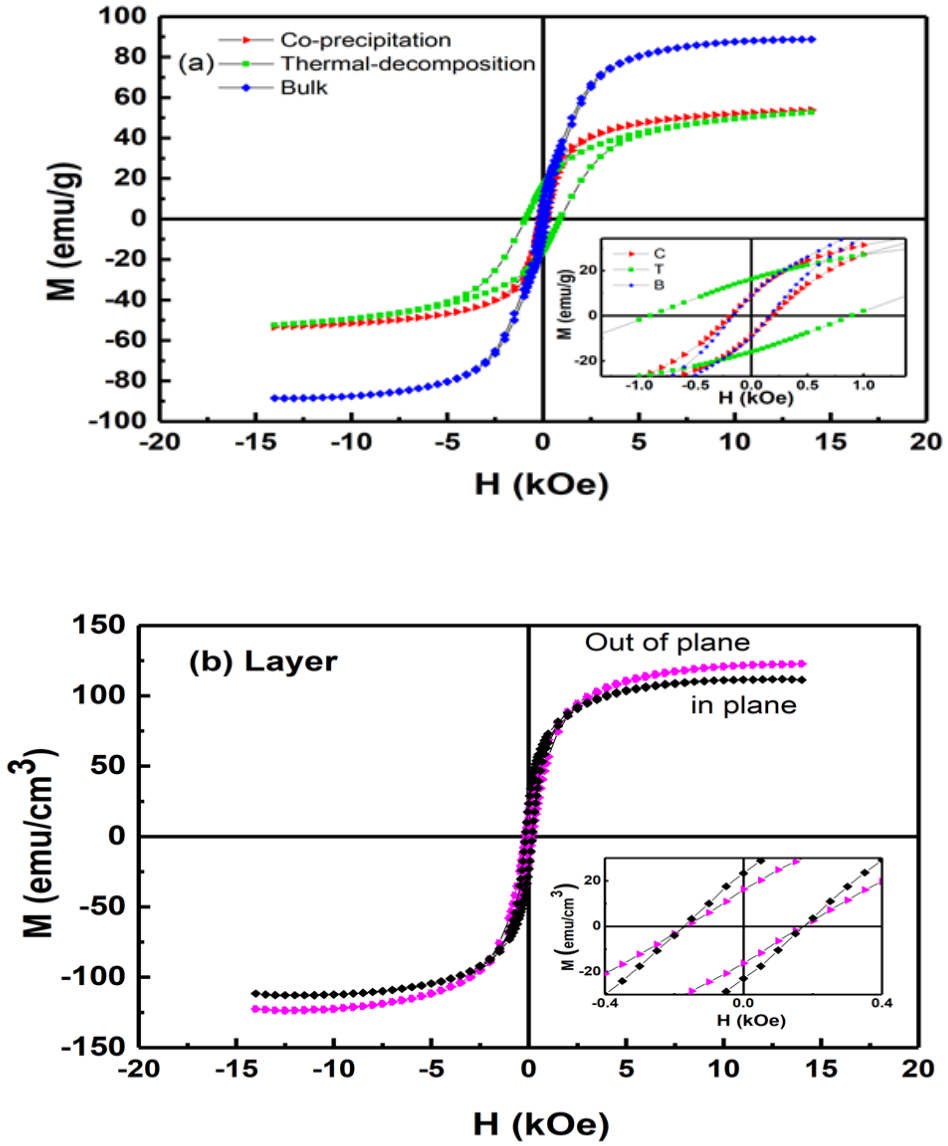

Fig. 4. Magnetic hysteresis loops of the $CoFe_2O_4$ samples at room temperature (300 K).

Table 2. The saturation magnetization (M_s), coercivity (H_c) and remanent magnetization of $CoFe_2O_4$ samples.

Parameter	**C**	**T**	**L**	**B**
t	0.98 (nm)	0.97 (nm)	-	-
M_s	53.81 (emu/g)	52.71 (emu/g)	122.70 (emu/cm^3)	88.77 (emu/g)
M_R	9.14 (emu/g)	16.18 (emu/g)	23.47 (emu/cm^3)	9.11 (emu/g)
H_C	179.98 (Oe)	893.99 (Oe)	173.53(Oe)	161.91 (Oe)

Table 3. The thickness of the dead layer of $CoFe_2O_4$ samples.

Parameter	**C**	**T**	**B**
Absorption wavelength (nm)	634	691	623
Band gap (eV)	3.38	3.76	3.01

3.3. Optical properties

The optical characteristics of co-precipitated nanoparticles samples and thermal decomposition and Bulk state were taken using visible-ultraviolet spectroscopy (UV-Vis) in the wavelength range between 250 and 700 nm at room temperature. The obtained results along with the energy gap diagram can be seen in Figures 5 (a-c). The absorption graphs of all $CoFe_2O_4$ samples show absorption in the visible light region, in the range of 600 to 700 nm. This absorption originates from the transition of Co^{2+} and Fe^{3+} electrical charges in the conduction band [37]. The energy gap was calculated using Tauc's equation [38, 39].

$$(\alpha h\nu)^2 = A(h\nu - Eg) \quad (6)$$

Where, α is the absorption coefficient, ν is the light frequency, A is a constant value, and E_g is the band gap value. The graph αhν is drawn in terms of hν, and is obtained by drawing a tangent line on the linear part of the band gap curve. The results are reported in Table 3. The energy gap is influenced by various factors such as the presence of impurities, particle size, and structural parameters [38]. According to the Table 3, the E_g value in nanoparticles is greater than that of the bulk sample. In addition, the nanoparticles prepared by thermal decomposition method has smaller E_g compared to the nanoparticles prepared by co-precipitation method. According to crystallite size (see Table 1), the T sample consist of smaller crystallites than C sample. This means that smaller particles will show larger E_g, and therefore the bulk sample shows the lowest band gap value.

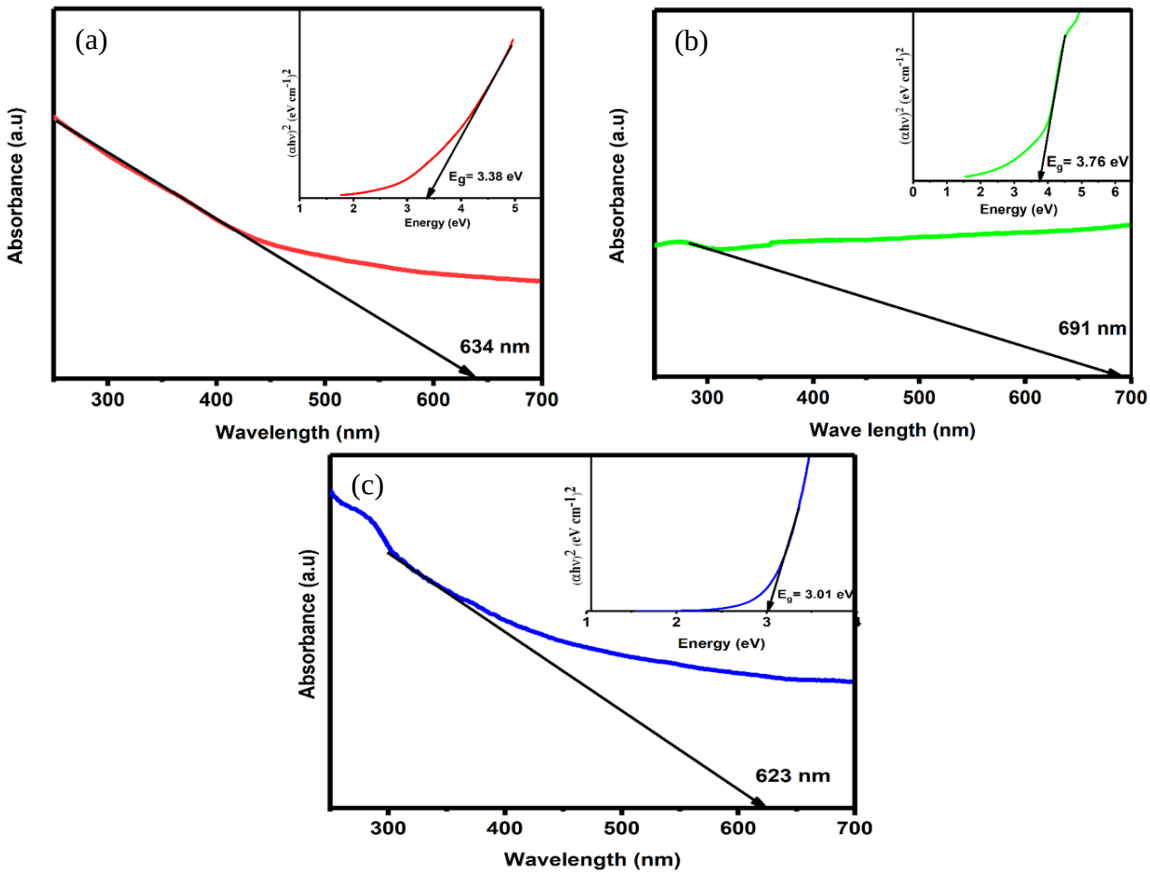

Fig. 5. UV-vis spectra and band-gap energy values of the samples.

4. Conclusion

The saturation magnetization for the bulk sample is higher than that of the nanoparticles and layer, which is due to the formation of a dead layer on the surface of the nanoparticles, and the layer. The highest coercivity value was obtained in thermal decomposition nanoparticles, the coercivity of other samples is lower. The optical properties were investigated and value of absorption wavelength in nanoparticle samples and bulk sample was obtained between 600-700 nm. The amount of band gap in nanoparticle samples was higher than that in the bulk sample.

References

[1] S.Y. Srinivasan, K.M. Paknikar, D. Bodas, V. Gajbhiye, "Applications of cobalt ferrite nanoparticles in biomedical nanotechnology." Nanomedicine 13 (2018) 1221-1238.

[2] S. Amiri, H. Shokrollahi, "The role of cobalt ferrite magnetic nanoparticles in medical science." Materials Science and Engineering: C 33 (2013) 1-8.

[3] K. Maaz, A. Mumtaz, S. Hasanain, A. Ceylan, "Synthesis and magnetic properties of cobalt ferrite ($CoFe_2O_4$) nanoparticles prepared by wet chemical route." Journal of magnetism and magnetic materials 308 (2007) 289-295.

[4] L. Phua, F. Xu, Y. Ma, C. Ong, "Structure and magnetic characterizations of cobalt ferrite films prepared by spray pyrolysis." Thin Solid Films 517 (2009) 5858-5861.

[5] A. Salunkhe, V. Khot, M.R. Phadatare, S. Pawar, "Combustion synthesis of cobalt ferrite nanoparticles—Influence of fuel to oxidizer ratio." Journal of alloys and compounds 514 (2012) 91-96.

[6] P.D. Thang, G. Rijnders, D.H. Blank, "Spinel cobalt ferrite by complexometric synthesis." Journal of magnetism and magnetic materials 295 (2005) 251-256.

[7] S.H. Xiao, W.F. Jiang, L.Y. Li, X.J. Li, "Low-temperature auto-combustion synthesis and magnetic properties of cobalt ferrite nanopowder." Materials Chemistry and Physics 106 (2007) 82-87.

[8] A. Ahlawat, V. Sathe, "Raman study of $NiFe_2O_4$ nanoparticles, bulk and films: effect of laser power." Journal of Raman Spectroscopy 42 (2011) 1087-1094.

[9] B. Aslibeiki, P. Kameli, M. Ehsani, "$MnFe_2O_4$ bulk, nanoparticles and film: A comparative study of structural and magnetic properties." Ceramics International 42 (2016) 12789-12795.

[10] E. Fitriyanti, B. Purnama, "Comparison XRD pattern of $CoFe_2O_4$ thin films and nanoparticles." Journal of Physics: Conference Series IOP Publishing (2017) 012010.

[11] B. Aslibeiki, P. Kameli, H. Salamati, "The effect of grinding on magnetic properties of agglomereted $MnFe_2O_4$ nanoparticles." Journal of magnetism and magnetic materials 324 (2012) 154-160.

[12] B. Aslibeiki, N. Eskandarzadeh, H. Jalili, A. Ghotbi Varzaneh, P. Kameli, I. Orue, V. Chernenko, A. Hajalilou, L.P. Ferreira, M.M. Cruz, "Magnetic hyperthermia properties of $CoFe_2O_4$ nanoparticles: Effect of polymer coating and interparticle interactions." Ceramics International 48 (2022) 27995-28005.

[13] B. Aslibeiki, P. Kameli, M.H. Ehsani, H. Salamati, G. Muscas, E. Agostinelli, V. Foglietti, S. Casciardi, D. Peddis, "Solvothermal synthesis of $MnFe_2O_4$ nanoparticles: The role of polymer coating on morphology and magnetic properties." Journal of Magnetism and Magnetic Materials 399 (2016) 236-244.

[14] B. Aslibeiki, P. Kameli, "Magnetic properties of $MnFe_2O_4$ nano-aggregates dispersed in paraffin wax." Journal of Magnetism and Magnetic Materials 385 (2015) 308-312.

[15] H. Jalili, B. Aslibeiki, A.G. Varzaneh, V.A. Chernenko, "The effect of magneto-crystalline anisotropy on the properties of hard and soft magnetic ferrite nanoparticles." Beilstein journal of nanotechnology 10 (2019) 1348-1359.

[16] B. Aslibeiki, P. Kameli, H. Salamati, G. Concas, M.S. Fernandez, A. Talone, G. Muscas, D. Peddis, "Co-doped $MnFe_2O_4$ nanoparticles: magnetic anisotropy and interparticle interactions." Beilstein journal of nanotechnology 10 (2019) 856-865.

[17] D. Erdem, N.S. Bingham, F.J. Heiligtag, N. Pilet, P. Warnicke, L.J. Heyderman, M. Niederberger, "$CoFe_2O_4$ and $CoFe_2O_4$-SiO_2 Nanoparticle Thin Films with Perpendicular Magnetic Anisotropy for Magnetic and Magneto-Optical Applications." Advanced Functional Materials 26 (2016) 1954-1963.

[18] B. Aslibeiki, Nanostructural, "magnetic and electrical properties of Ag doped Mn-ferrite nanoparticles." Current Applied Physics 14 (2014) 1659-1664.

[19] B. Aslibeiki, P. Kameli, "Effect of ZnO on Structural and Magnetic Properties of $MnFe_2O_4$/ZnO Nanocomposite." Journal of Superconductivity and Novel Magnetism 28 (2015) 3343-3350.

[20] E. Fantechi, G. Campo, D. Carta, A. Corrias, C. de Julián Fernández, D. Gatteschi, C. Innocenti, F. Pineider, F. Rugi, C. Sangregorio, "Exploring the effect of Co doping in fine maghemite nanoparticles." The Journal of Physical Chemistry C 116 (2012) 8261-8270.

[21] L. Hu, C. de Montferrand, Y. Lalatonne, L. Motte, A. Brioude, "Effect of cobalt doping concentration on the crystalline structure and magnetic properties of monodisperse $Co_xFe_{3-x}O_4$ nanoparticles within nonpolar and aqueous solvents." The Journal of Physical Chemistry C 116 (2012) 4349-4355.

[22] X. Li, C. Kutal, "Synthesis and characterization of superparamagnetic $Co_xFe_{3-x}O_4$ nanoparticles." Journal of alloys and compounds 349 (2003) 264-268.

[23] P. Prieto, J.F. Marco, J.E. Prieto, S. Ruiz-Gomez, L. Perez, P. Rafael, M. Vázquez, J. de la Figuera, "Epitaxial integration of $CoFe_2O_4$ thin films on Si (001) surfaces using TiN buffer layers." Applied Surface Science 436 (2018) 1067-1074.

[24] G.C. Lavorato, E. Lima Jr, D. Tobia, D. Fiorani, H.E. Troiani, R.D. Zysler, E.L. Winkler, "Size effects in bimagnetic $CoO/CoFe_2O_4$ core/shell nanoparticles." Nanotechnology 25 (2014) 355704.

[25] B. Aslibeiki, "Magnetic interactions and hysteresis loops study of $Co/CoFe_2O_4$ nanoparticles." Ceramics International 42 (2016) 6413-6421.

[26] M.H. Habibi, H.J. Parhizkar, "FTIR and UV–vis diffuse reflectance spectroscopy studies of the wet chemical (WC) route synthesized nano-structure $CoFe_2O_4$ from $CoCl_2$ and $FeCl_3$." Spectrochimica Acta Part A: Molecular and Biomolecular Spectroscopy 127 (2014) 102-106.

[27] V. Jeseentharani, M. George, B. Jeyaraj, A. Dayalan, K. Nagaraja, "Synthesis of metal ferrite (MFe_2O_4, M= Co, Cu, Mg, Ni, Zn) nanoparticles as humidity sensor materials." Journal of experimental nanoscience 8 (2013) 358-370.

[28] H. Nikmanesh, P. Kameli, S.M. Asgarian, S. Karimi, M. Moradi, Z. Kargar, J. Ventura, B. Bordalo, H. Salamati, "Positron annihilation lifetime, cation distribution and magnetic features of $Ni_{1-x}Zn_xFe_{2-x}Co_xO_4$ ferrite nanoparticles." RSC Advances 7 (2017) 22320-22328.

[29] H. Wang, J. Huang, L. Ding, D. Li, Y. Han, "A facile synthesis of monodisperse $CoFe_2O_4/SiO_2$ nanoparticles." Applied surface science 257 (2011) 7107-7112.

[30] J. Zhang, J. Wan, S. Huang, J. Du, J. Zhu, D. Zhang, Q. Yin, Y. Wu, "Solvothermal synthesis and magnetic property of magnetic chains self-assembled by Fe_3O_4 microoctahedrons." Chinese Journal of Chemistry 28 (2010) 1607-1612.

[31] P. Dutta, S. Pal, M. Seehra, N. Shah, G. Huffman, "Size dependence of magnetic parameters and surface disorder in magnetite nanoparticles." Journal of Applied Physics 105 (2009) 07B501.

[32] D. Sharma, N. Khare, "Tailoring the optical bandgap and magnetization of cobalt ferrite thin films through controlled zinc doping." AIP Advances 6 (2016) 085005.

[33] A. Sathya, P. Guardia, R. Brescia, N. Silvestri, G. Pugliese, S. Nitti, L. Manna, T. Pellegrino, "$Co_xFe_{3-x}O_4$ nanocubes for theranostic applications: effect of cobalt content and

particle size." Chemistry of Materials 28 (2016) 1769-1780.
[34] H. Jalili, B. Aslibeiki, A. Hajalilou, O. Musalu, L.P. Ferreira, M.M. Cruz, "Bimagnetic hard/soft and soft/hard ferrite nanocomposites: Structural, magnetic and hyperthermia properties." Ceramics International 48 (2022) 4886-4896.
[35] B. Aslibeiki, G. Varvaro, D. Peddis, P. Kameli, "Particle size, spin wave and surface effects on magnetic properties of $MgFe_2O_4$ nanoparticles." Journal of Magnetism and Magnetic Materials 422 (2017) 7-12.
[36] B. Aslibeiki, P. Kameli, H. Salamati, "Nanomagnetism." Iranian Journal of Physics Research 16 (2019) 251-272.
[37] M. Lenglet, F. Hochu, J. Dürr, "Optical properties of mixed cobalt ferrites." Le Journal de Physique IV 7 (1997) C1-259-C251-260.
[38] G. Pandey, S. Dixit, "Growth mechanism and optical properties determination of CdS nanostructures." The Journal of Physical Chemistry C 115 (2011) 17633-17642.
[39] R. Torkamani, B. Aslibeiki, H. Naghshara, M. Darbandi, "Structural and optical properties of ZnO nanorods: The effect of concentration and pH of the growth solution." Optical Materials 127 (2022) 112295.